Humidity insensitive TOPAS polymer fiber Bragg grating sensor

Wu Yuan,[1] Lutful Khan,[2] David J. Webb,[2,*] Kyriacos Kalli,[3] Henrik K. Rasmussen,[4] Alessio Stefani,[1] Ole Bang[1]

[1]*DTU Fotonik, Dept. of Photonics Engineering, Technical University of Denmark, DK-2800 Kgs. Lyngby, Denmark*
[2]*Photonic Research Group, Aston University, Aston Triangle, Birmingham, B4 7ET, UK*
[3]*Nanophotonics Research Laboratory, Cyprus University of Technology, Cyprus*
[4]*Dept. of Mechanical Engineering, Technical University of Denmark DK-2800 Kgs. Lyngby, Denmark*
**d.j.webb@aston.ac.uk*

Abstract: We report the first experimental demonstration of a humidity insensitive polymer optical fiber Bragg grating (FBG), as well as the first FBG recorded in a TOPAS polymer optical fiber in the important low loss 850nm spectral region. For the demonstration we have fabricated FBGs with resonance wavelength around 850 nm and 1550 nm in single-mode microstructured polymer optical fibers made of TOPAS and the conventional poly (methyl methacrylate) (PMMA). Characterization of the FBGs shows that the TOPAS FBG is more than 50 times less sensitive to humidity than the conventional PMMA FBG in both wavelength regimes. This makes the TOPAS FBG very appealing for sensing applications as it appears to solve the humidity sensitivity problem suffered by the PMMA FBG.

OCIS codes: (060.2370) Fiber optics sensors; (060.2270) Fiber characterization; (050.2770) Gratings; (160.5470) Polymers.

References and links

1. H. Dobb, K. Carroll, D. J. Webb, K. Kalli, M. Komodromos, C. Themistos, G. D. Peng, A. Argyros, M. C. J. Large, M. A. van Eijkelenborg, Q. Fang, and I. W. Boyd, "Grating based devices in polymer optical fibre," Proc. SPIE 618901 (2006).
2. W. Yuan, A. Stefani, M. Bache, T. Jacobsen, B. Rose, N. Herholdt-Rasmussen, F. K. Nielsen, S. Andresen, O. B. Sørensen, K. S. Hansen, and O. Bang, "Improved thermal and strain performance of annealed polymer optical fiber Bragg gratings," Opt. Commun. **284**(1), 176–182 (2011).
3. G. Emiliyanov, J. B. Jensen, O. Bang, P. E. Hoiby, L. H. Pedersen, E. M. Kjaer, and L. Lindvold, "Localized biosensing with Topas microstructured polymer optical fiber," Opt. Lett. **32**(5), 460–462 (2007).
4. G. Emiliyanov, J. B. Jensen, O. Bang, P. E. Hoiby, L. H. Pedersen, E. M. Kjaer, and L. Lindvold, "Localized biosensing with TOPAS microstructured polymer optical fiber: Erratum," Opt. Lett. **32**(9), 1059 (2007).
5. G. E. Town, W. Yuan, R. McCosker, and O. Bang, "Microstructured optical fiber refractive index sensor," Opt. Lett. **35**(6), 856–858 (2010).
6. C. Markos, W. Yuan, K. Vlachos, G. E. Town, and O. Bang, "Label-free biosensing with high sensitivity in dual-core microstructured polymer optical fibers," Opt. Express **19**(8), 7790–7798 (2011).
7. W. Yuan, G. E. Town, and O. Bang, "Refractive index sensing in an all-solid twin-core photonic bandgap fiber," IEEE Sens. J. **10**(7), 1192–1199 (2010).
8. F. M. Cox, A. Argyros, and M. C. J. Large, "Liquid-filled hollow core microstructured polymer optical fiber," Opt. Express **14**(9), 4135–4140 (2006).
9. J. Jensen, P. Hoiby, G. Emiliyanov, O. Bang, L. Pedersen, and A. Bjarklev, "Selective detection of antibodies in microstructured polymer optical fibers," Opt. Express **13**(15), 5883–5889 (2005).
10. A. Dupuis, N. Guo, Y. Gao, N. Godbout, S. Lacroix, C. Dubois, and M. Skorobogatiy, "Prospective for biodegradable microstructured optical fibers," Opt. Lett. **32**(2), 109–111 (2007).
11. B. Hadimioglu and B. T. Khuri-Yakub, "Polymer Films as Acoustic Matching Layers," Ultrasonics Symposium, Proceedings IEEE, 3, 1337–1340 (1990).
12. Z. Xiong, G. D. Peng, B. Wu, and P. L. Chu, "Highly tunable Bragg gratings in single-mode polymer optical fibres," IEEE Photon. Technol. Lett. **11**(3), 352–354 (1999).
13. A. Stefani, W. Yuan, C. Markos, and O. Bang, "Narrow bandwidth 850 nm fiber Bragg gratings in few-mode polymer optical fibers," IEEE Photon. Technol. Lett. **23**(10), 660–662 (2011).

#151392 - $15.00 USD Received 19 Jul 2011; revised 5 Sep 2011; accepted 6 Sep 2011; published 23 Sep 2011

14. C. Zhang, W. Zhang, D. J. Webb, and G. D. Peng, "Optical fibre temperature and humidity sensor," Electron. Lett. **46**(9), 643–644 (2010).
15. N. G. Harbach, "Fiber Bragg gratings in polymer optical fibers," PhD Thesis, Lausanne, EPFL (2008).
16. H. Dobb, D. J. Webb, K. Kalli, A. Argyros, M. C. J. Large, and M. A. van Eijkelenborg, "Continuous wave ultraviolet light-induced fiber Bragg gratings in few- and single-mode microstructured polymer optical fibers," Opt. Lett. **30**(24), 3296–3298 (2005).
17. I. P. Johnson, K. Kalli, and D. J. Webb, "827nm Bragg grating sensor in multimode microstructured polymer optical fiber," Electron. Lett. **46**(17), 1217–1218 (2010).
18. I. P. Johnson, W. Yuan, A. Stefani, K. Nielsen, H. K. Rasmussen, L. Khan, D. J. Webb, K. Kalli, and O. Bang, "Optical fibre Bragg grating recorded in TOPAS cyclic olefin copolymer," Electron. Lett. **47**(4), 271–272 (2011).
19. Y. Tsuchida, K. Saitoh, and M. Koshiba, "Design of single-moded holey fibers with large-mode-area and low bending losses: the significance of the ring-core region," Opt. Express **15**(4), 1794–1803 (2007).
20. D. J. Webb, K. Kalli, K. Carroll, C. Zhang, M. Komodromos, A. Argyros, M. Large, G. Emiliyanov, O. Bang, and E. Kjaer, "Recent developments of Bragg gratings in PMMA and TOPAS polymer optical fibers," Advanced Sensor Systems and Applications III, Proc. of SPIE **6830**, 683002 (2007).
21. D. J. Webb, K. Kalli, C. Zhang, M. Komodromos, A. Argyros, M. Large, G. Emiliyanov, and O. Bang, "E, Kjaer, "Temperature sensitivity of Bragg gratings in PMMA and TOPAS microstructured polymer optical fibres," Photonic Crystal Fibers **II**, L9900 (2008).
22. www.topas.com.
23. G. Khanarian and H. Celanese, "Optical properties of cyclic olefin copolymers," Opt. Eng. **40**(6), 1024–1029 (2001).
24. K. Nielsen, H. K. Rasmussen, A. J. L. Adam, P. C. M. Planken, O. Bang, and P. U. Jepsen, "Bendable, low-loss Topas fibers for the terahertz frequency range," Opt. Express **17**(10), 8592–8601 (2009).
25. M. C. J. Large, L. Poladian, G. Barton, and M. A. van Eijkelenborg, "Microstructured polymer optical fibres," Springer, (2008).
26. M. A. van Eijkelenborg, M. C. J. Large, A. Argyros, J. Zagari, S. Manos, N. A. Issa, I. Bassett, S. Fleming, R. C. McPhedran, C. M. de Sterke, and N. A. P. Nicorovici, "Microstructured polymer optical fibre," Opt. Express **9**(7), 319–327 (2001).
27. N. A. Mortensen, "Semianalytical approach to short-wavelength dispersion and modal properties of photonic crystal fibers," Opt. Lett. **30**(12), 1455–1457 (2005).
28. G. D. Marshall, D. J. Kan, A. A. Asatryan, L. C. Botten, and M. J. Withford, "Transverse coupling to the core of a photonic crystal fiber: the photo-inscription of gratings," Opt. Express **15**(12), 7876–7887 (2007).
29. L. Rindorf and O. Bang, "Sensitivity of photonic crystal fiber grating sensors: biosensing, refractive index, strain, and temperature sensing," J. Opt. Soc. Am. B **25**(3), 310 (2008).

1. Introduction

Fiber Bragg gratings (FBGs) in polymer optical fiber (POF) are attractive for optical fiber sensing applications that measure strain and temperature due to their low Young's modulus (25 times lower than silica), their high thermo-optic coefficient, and because they can be stretched far more than silica fibers before breaking (in excess of 10%) [1,2]. In addition, polymer optical fibers (POFs) are clinically acceptable, which along with their flexible and non-brittle nature makes POFs important candidates for in-vivo biosensing applications [3–10]. A recent important application to photo-acoustic imaging has been demonstrated, which takes advantage of the low Young's modulus and the fact that polymers are, in general, much better impedance matched to water than glass fibers [11]. Fiber Bragg gratings have been reported in both step index POFs [2,12–15] and microstructured POFs (mPOFs) [13,16–18]. Microstructured optical fibers have a cladding consisting of a pattern of air holes that extend for the full length of the fiber and the optical properties can be designed by adjusting the relative position, size and shape of the air holes. Such mPOFs have the advantage that they easily can be made endlessly single-mode, i.e., single-mode at all frequencies, even when the core is large [19]. Furthermore, the holes of the mPOF can be used to hold a gas or a biological sample, which can then be studied by evanescent-wave sensing with a strong overlap between the electric field and the holes [3,4,9].

The majority of POFs to date are based on PMMA. Monomer residues inside PMMA, and its aptitude for water absorption often make the drawing process with PMMA preforms problematic, and PMMA based FBG strain sensors have a significant cross-sensitivity to humidity [15,18,20,21]. These problems might be reduced by using other polymer materials, such as TOPAS, which is a cyclic olefin copolymer [22]. TOPAS has no monomers and its moisture absorption is reported to be at least 30 times lower than PMMA [23]. Furthermore, although TOPAS is chemically inert and bio-molecules do not readily bind to its surface,

#151392 - $15.00 USD Received 19 Jul 2011; revised 5 Sep 2011; accepted 6 Sep 2011; published 23 Sep 2011

treatment with antraquinon and subsequent UV activation allows sensing molecules to be deposited in well defined spatial locations [3,4]. When combined with grating technology this provides considerable potential for label-free bio-sensing [18]. In addition, TOPAS is also an ideal material for fabricating low-loss terahertz fibers [24].

Despite their promise, no commercial application of POF FBGs has been realized as yet, primarily due to the high material loss of both PMMA and TOPAS mPOFs in the 1300-1600 nm spectral region. A considerable decrease in the material loss from approximately 100 dB/m to 1 dB/m is achievable by working at a lower wavelength [23,25]. In this paper we therefore address two important problems for the application of POF FBGs: We fabricate and characterize the first FBGs in single-mode TOPAS mPOFs in the lower loss window around 800-900 nm and we use these FBGs to further demonstrate humidity insensitive operation due the properties of the base material TOPAS. The humidity measurements are carried out for both of the important sensing wavelengths 850 nm and 1550 nm.

Specifically, we use the phase-mask technique and a 325 nm HeCd laser to write several FBGs around 800-900 nm in TOPAS mPOFs. The same technique was used previously to fabricate a TOPAS grating with a resonance wavelength of 1567.9 nm [18], The static tensile strain sensitivity and the temperature sensitivity of an 870 nm TOPAS grating have been measured to be 0.64 pm/μstrain and −78 pm/°C, respectively. The relatively low material loss of the fiber at this wavelength, compared to that at longer wavelengths, will considerably enhance the potential utility of the TOPAS FBG, just as for PMMA, in which an FBG was recently written at 827 nm [17] and 850 nm [13]. It is also convenient to work at 850 nm, because CMOS technology can potentially provide interrogation systems that are even cheaper than those at the C and L band. Furthermore, the characterization reported here shows a humidity sensitivity of below 0.7 pm/% for both 850 nm and 1550 nm TOPAS FBGs, the value being actually limited by the 0.3 °C temperature stability of the environmental chamber used for the tests. This is more than 50 times lower than the 38 pm/% reported for a 1565 nm PMMA FBG [14]. The low affinity for water makes TOPAS FBGs very good candidates to address the humidity sensitivity problem suffered by PMMA FBGs, which has so far compromised their suitability for long term strain monitoring.

2. Experiments

2.1 TOPAS mPOFs and FBG writing

The drill-and-draw technique [25,26], was used for the fabrication of the mPOFs. The material used for the TOPAS mPOFs was a TOPAS® cyclic olefin copolymer in the form of granulates of the particular grade 8007, obtained from TOPAS Advanced Polymers, Inc. The TOPAS granulates were cast into 6 cm diameter rods and the desired hexagonal hole structure was drilled into the rod with a 3 mm diameter drill. This structure was preserved throughout the drawing process. The preforms were then drawn to fiber by first drawing a 5 mm cane, which was then sleeved and drawn again. The TOPAS mPOF used in our experiment was drawn without pressure and with low tension. The resulting mPOF has a diameter of 240 μm and a solid core surrounded by two rings of air holes arranged in a hexagonal lattice. The air-hole diameter is on average 2±0.2 μm and the inter-hole pitch is on average 6±0.2 μm, respectively, as shown in Fig. 1. The Topas mPOF has a hole diameter to pitch ratio of $d/\Lambda \approx 0.33$, which is well below the threshold of 0.42 that ensures endlessly single-mode operation of microstructued optical fibers of arbitrary base material [27].

#151392 - $15.00 USD Received 19 Jul 2011; revised 5 Sep 2011; accepted 6 Sep 2011; published 23 Sep 2011

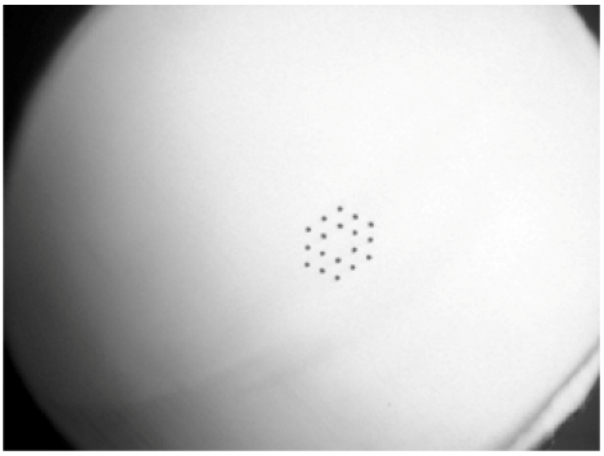

Fig. 1. The microscope image of the end facet of our TOPAS mPOF.

The gratings were inscribed using a 30 mW CW HeCd laser operating at 325 nm (IK5751I-G, Kimmon). The fiber was supported by v-grooves on both sides with a gap in between to avoid reflection, and it was taped down to ensure that the fiber did not sag. A circular Gaussian laser beam was expanded from diameter 1.2 mm to 1.2 cm in one direction along the fiber by a cylindrical lens. The laser beam was then focused vertically downwards into the fiber core using another cylindrical lens to expose the fiber through a phasemask customized for 325 nm writing with a uniform period of 572.4 nm (Ibsen Photonics), which was originally designed for 850 nm grating inscription in PMMA. A grating length of 10 mm was defined by an aperture underneath the focus lens to control the beam width. The laser irradiance at the fiber was about 5 Wcm^{-2}. The resulting grating wavelength was around 870 nm, with the longer resonance wavelength compared to that in PMMA fiber being due to the higher refractive index $n \approx 1.53$ of TOPAS at 800 nm.

The growth of the 10 mm gratings was monitored in reflection with a spectral resolution of 0.01 nm during the inscription using an 850 nm silica fiber circulator, a SuperK Versa broadband source (NKT Photonics) and an optical spectrum analyzer (Ando AQ6317B). A standard single-mode silica fiber was butt-coupled to the mPOF using an angle cleaved end-facet and a small amount of refractive index matching gel in order to reduce Fresnel reflections, which manifested themselves as background noise. The ends of the mPOF were prepared using a homemade hot blade cleaver equipped with flat side blade with a temperature of 50 °C for both the blade and fiber, which gives a high quality end facet. Typical reflection spectra of a 10 mm grating fabricated in the TOPAS mPOF with different exposure times are shown in Fig. 2(a). The necessary exposure time to write a FBG in an mPOF is longer than to write a grating in a solid step-index POF of the same diameter. This is because the holes around the core of the mPOF scatter a significant part of the laser power during the writing process [28], and that is why we only used two rings of air holes in our TOPAS mPOF. We further observed that side-lobes appeared in the reflection spectrum after 236 minutes.

The growth dynamics of the gratings, i.e. the time dependent peak intensity and grating bandwidth, are shown in Fig. 2(b). The grating writing dynamics initially displays a growth in strength accompanied by an almost constant grating bandwidth. After a certain threshold time, which was around 300 minutes, the grating strength begins to saturate. The bandwidth is less than 0.34 nm and thus we do not need to take it into account when we investigate the sensitivity of the FBG [29].

#151392 - $15.00 USD Received 19 Jul 2011; revised 5 Sep 2011; accepted 6 Sep 2011; published 23 Sep 2011

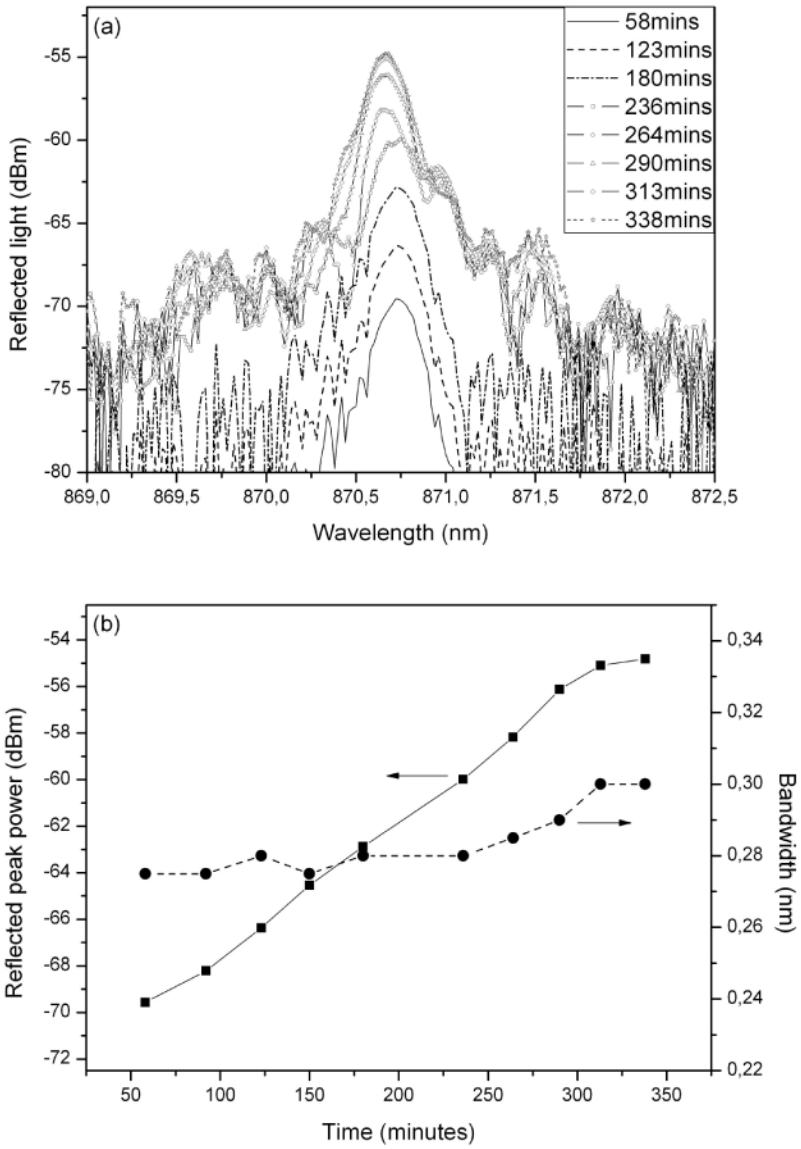

Fig. 2. (a) Reflection spectra (spectral resolution 0.01 nm) of the 10 mm FBG in a TOPAS mPOF at different writing times. (b) Growth dynamic of the peak intensity and bandwidth of the 10 mm FBG during writing.

2.2 Strain and temperature characterization of TOPAS mPOF FBGs

The strain tuning of the 870 nm FBG was investigated by mechanical stretching. The two ends of the mPOF were glued to two micro-translation stages with epoxy glue (Loctite 3430), with one of them fixed and used to butt-couple the mPOF to a silica single mode fiber. The epoxy glue is mechanically much stiffer than the TOPAS mPOF, so that it does not unduly influence the strain. The other stage can move longitudinally to apply axial strain to the grating manually with a low loading speed. The axial strain values were determined by dividing the fiber longitudinal elongation by the length of fiber between the two gluing points. The longitudinal displacement accuracy of the moving translation stage is 0.01 mm. The gratings were left to stabilize for about ten minutes each time the tensile strain was changed

#151392 - $15.00 USD Received 19 Jul 2011; revised 5 Sep 2011; accepted 6 Sep 2011; published 23 Sep 2011

before reading the reflection spectrum. A strain loading experiment was carried out to study the strain tuning response of the grating, as shown in Fig. 3(a). The fiber was gradually stretched to 2.17% strain. The grating shows a linear response of the wavelength shift over the whole strain loading range and a linear fit of the results gives a strain sensitivity of 0.64±0.04 pm/μstrain, which is similar to the reported sensitivities of 0.71 pm/μstrain of PMMA mPOF FBGs at 827nm [17] and 850nm [13].

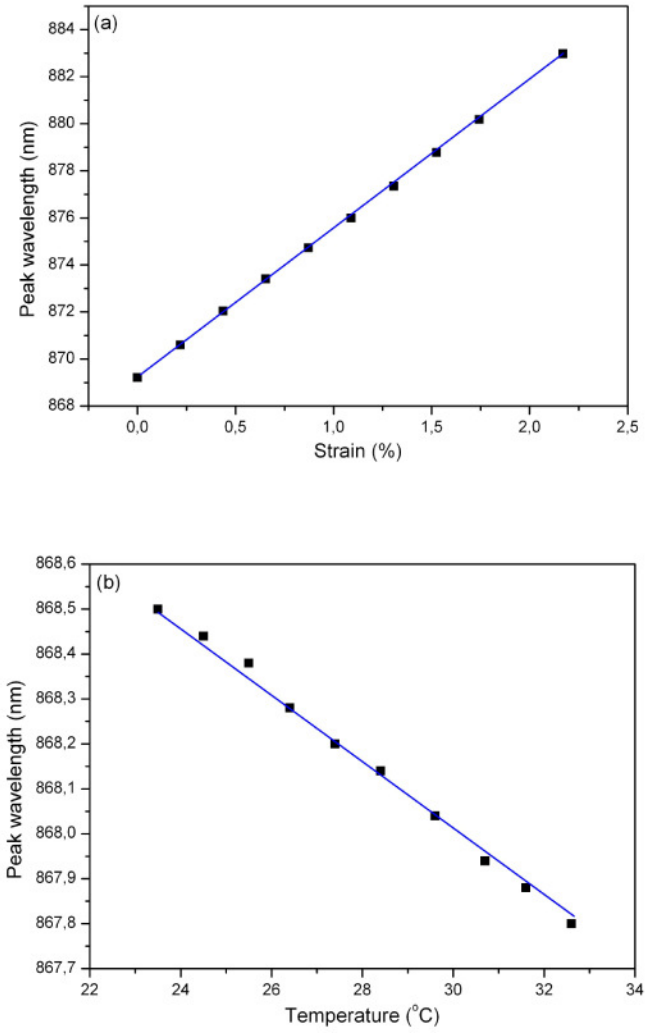

Fig. 3. Strain (a) and temperature (b) response of the 10mm TOPAS mPOF FBG, giving sensitivities of 0.64±0.04 pm/μstrain and −78±1 pm/°C, respectively.

The temperature response of the gratings was also studied with the same monitoring setup as the one used during the grating inscription. The polymer fiber was heated up with a resistive hot stage (MC60+TH60, Linkam). A thermo coupler was used to measure the temperature as close to the grating as possible with an uncertainty around 0.3°C. One end of the mPOF was clamped and butt-coupled to a silica fiber circulator, and the entire length of the mPOF with grating was attached to the surface of the heater by several layers of lens papers on the top. Twenty minutes was allowed for the temperature of the grating to stabilize at each new setting before readings of the resonance wavelengths and peak intensity were taken. The grating was heated up from room temperature to 32.6°C stepwise in a single cycle, as shown in Fig. 3(b). A blue shift of the resonance wavelength was indentified during the

#151392 - $15.00 USD Received 19 Jul 2011; revised 5 Sep 2011; accepted 6 Sep 2011; published 23 Sep 2011

heating up process, but no obvious bandwidth change was found. A temperature sensitivity of −78±1 pm/°C was found for this grating by a linear fit. In contrast, a temperature sensitivity of −36.5 pm/°C was reported for a 1567.9 nm FBG in a 2-ring TOPAS mPOF before [18]. The fiber used in [18] had a slightly larger diameter of 287 µm, larger holes with a diameter of 3.8 µm, and a larger pitch of 8.5 µm. The larger relative hole size of 0.44 (compared to the 0.33 of the fiber we use here) could be what shields against a temperature increase in the core and thereby gives a weaker temperature sensitivity if the fiber is not left to stabilize at each temperature setting. The difference is currently under investigation. The negative temperature sensitivity means that the negative thermo-optic coefficient of approximately -1×10^{-4}/°C [23], dominates the positive thermo-expansion coefficient of approximately $+6\times10^{-5}$/°C [23], in the thermal response of the TOPAS mPOF FBG, which is similar to the case of the PMMA FBG [2]. This corrects earlier preliminary results that showed a strong positive response of a TOPAS FBG [20,21]. The FBG reported here has a clear reflection spectrum, whereas the earlier measurement showed an FBG that could only be measured in transmission [21], which is most probably the explanation of the earlier result.

2.2 Humidity characterization of TOPAS mPOF FBGs

Research to date on POF gratings has essentially involved PMMA, which has an affinity for water. When PMMA FBGs are applied to temperature and strain sensing, an important issue is the cross-sensitivity to humidity. In contrast, TOPAS has a much lower moisture absorption uptake, i.e., <0.01% [23], and this property makes it a very appealing alternative to address the humidity sensitivity problem suffered by PMMA, which has a moisture absorption uptake of 0.3% [23]. After inscribing the 870 nm grating in the TOPAS mPOF, a second phase mask was then used to enable the fabrication of a grating in the same mPOF with a smaller Bragg wavelength that is more compatible with the available light sources and detectors at 850 nm. The same TOPAS mPOF was also used in the inscription of a Bragg grating with a resonance wavelength of ~1568 nm for studying the humidity response of the TOPAS FBG in the L band.

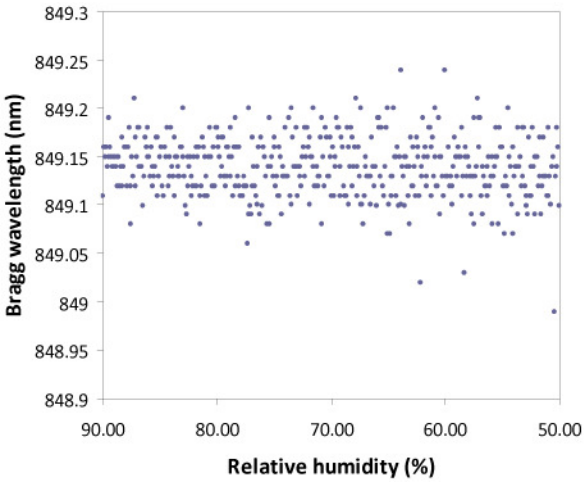

Fig. 4. , Humidity response of an 849 nm TOPAS mPOF FBG. The humidity was continuously decreased from 90% to 50% over a 4 hour time period.

As shown in Fig. 4, a TOPAS mPOF FBG with a resonance peak of ~849 nm has been examined in an environmental chamber (Sanyo Gallenkamp) for 4 hours at 25 °C, where it was subject to a humidity gradually decreasing from 90% to 50% over that period. Linear regression provides a slope of 0.26±0.12 pm/%, which means that over this humidity range a shift of the mean resonance peak of only about −10 pm was found. Caution must however be exercised in interpreting this wavelength shift because the environmental chamber has a

#151392 - $15.00 USD Received 19 Jul 2011; revised 5 Sep 2011; accepted 6 Sep 2011; published 23 Sep 2011

specified temperature stability of 0.3 °C. Given the measured temperature sensitivity of the FBG quoted earlier, a 0.3 °C temperature rise would cause a wavelength shift of −18pm, which is rather larger than the −10pm average shift observed in the data of Fig. 4. Consequently, we cannot conclude that the observed wavelength shift is due to humidity change as it may be simply due to temperature drifts in the chamber. All we can do is to calculate an upper limit on the magnitude of any humidity sensitivity. We do this using a worst-case scenario where we assume that there has been a negative temperature change of 0.3 °C over the course of the experiment, leading to a temperature induced positive wavelength shift of 18pm; the observed net negative wavelength shift of −10pm would therefore require a contribution to wavelength shift from humidity of −28pm over the experiment or 0.7 pm/% relative humidity. We must stress that this is a worst case calculation and the actual sensitivity is likely to be lower. As a comparison, a PMMA based FBG at 1565nm displayed a sensitivity of 38.4±0.4 pm/% relative humidity [14], which is over 50 times more than the maximum possible humidity sensitivity of the TOPAS FBG studied here.

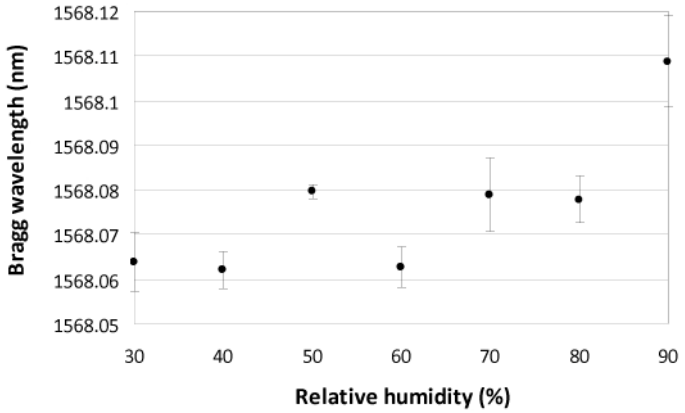

Fig. 5. Variation of the Bragg wavelength of a 1568 nm TOPAS FBG with humidity from 30% to 90%.

Following the humidity test carried out on the 849 nm TOPAS FBG, a second test was run to determine the humidity sensitivity of TOPAS using a 1568 nm FBG. Unlike the previous test, the environmental chamber was this time set to increase humidity stepwise from 30% to 90% at 25°C with 10% increments and a duration of two hours for each step. Spectral data were obtained every 30 seconds at each humidity, following a 30 minute acclimatisation period; the average value and associated error are plotted in Fig. 5. Linear regression of the humidity response gives a sensitivity of –0.59±0.02 pm/% relative humidity, with a shift of 36 pm over the humidity range studied. However, once again the measurement is effectively limited by the 0.3°C stability of the oven as a temperature drift of such magnitude could produce a shift of 33 pm over the course of the experiment. The measured sensitivity is nevertheless already 65 times smaller than for an equivalent FBG in PMMA based fiber [14]. Previous studies already showed that the high and positive humidity sensitivity of the PMMA grating was due to the swelling of the fibre and the increase of refractive index, both of which were caused by the high moisture uptake of the material [14, 15, 23].

3. Conclusions

We have demonstrated for the first time the inscription of FBGs in TOPAS mPOFs with resonance wavelengths within 800-900 nm. The relatively low material loss of the fiber at this wavelength compared to that at longer wavelengths, together with the convenient accessibility of the cost-effective CMOS technology at this wavelength, will considerably enhance the potential utility of the TOPAS FBGs. The static tensile and thermal characterization of an 870 nm TOPAS grating showed the strain sensitivity and the temperature sensitivity to be 0.64

#151392 - $15.00 USD Received 19 Jul 2011; revised 5 Sep 2011; accepted 6 Sep 2011; published 23 Sep 2011

pm/μstrain and −78 pm/°C, respectively. Furthermore, we determined for the first time that the humidity sensitivity of the TOPAS FBG was more than 50 times less than that of PMMA FBGs, which makes TOPAS FBGs better candidates for long-term monitoring of strain and temperature with negligible cross-sensitivity to humidity.

Acknowledgements

We would like to acknowledge support from the Danish National Advanced Technology Foundation.

#151392 - $15.00 USD Received 19 Jul 2011; revised 5 Sep 2011; accepted 6 Sep 2011; published 23 Sep 2011